iScience, Volume *23*

Supplemental Information

Titanium Tackles the Endoplasmic Reticulum: A First Genomic Study on a Titanium Anticancer Metallodrug

Maya Miller, Anna Mellul, Maya Braun, Dana Sherill-Rofe, Emiliano Cohen, Zohar Shpilt, Irene Unterman, Ori Braitbard, Jacob Hochman, Edit Y. Tshuva, and Yuval Tabach

Supplemental Information

PhenolaTi

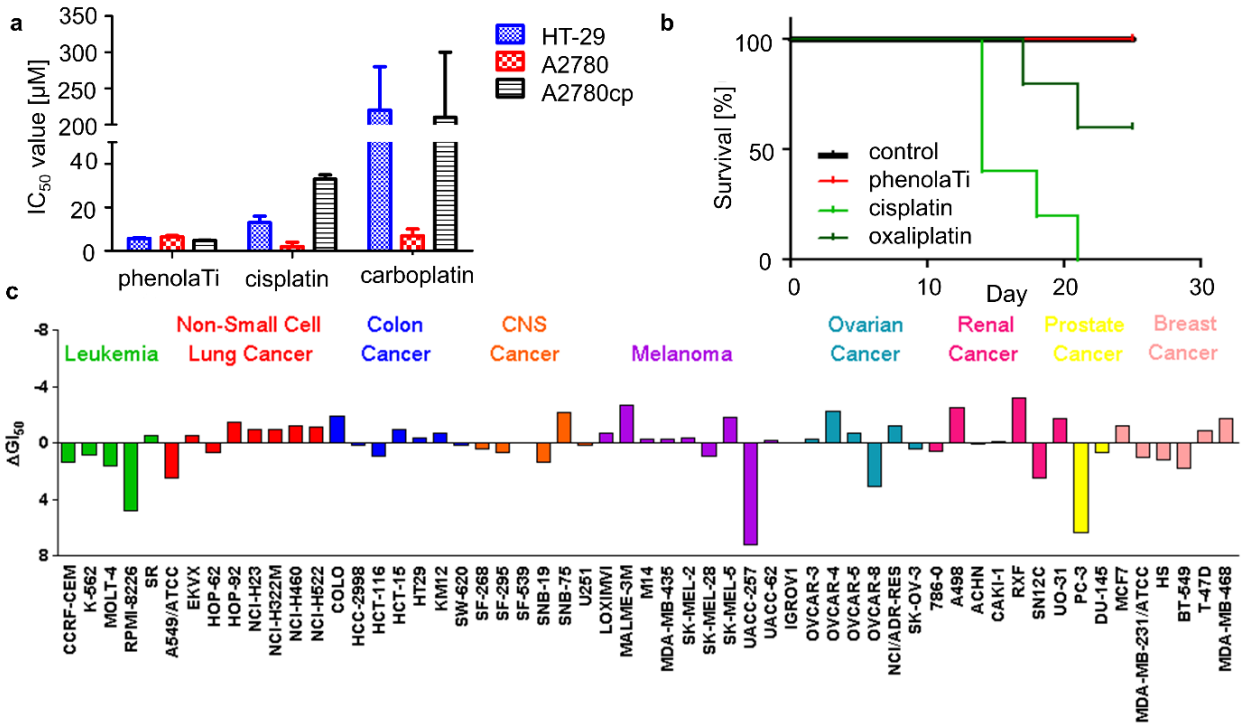

Figure S1: PhenolaTi is a lead anticancer metallodrug. Related to Scheme 1. (a) Relative IC_{50} values (µM) towards HT-29, A2780 and A2780cp (cisplatin resistant) human cancer cell lines of phenolaTi, cisplatin and carboplatin (Meker et al., 2016) (after 72 hours of incubation) (b) *In vivo* effect of phenolaTi (1.6 mg/kg), cisplatin (5 mg/kg), and oxaliplatin (5 mg/kg) on survival of Balb/c mice (Ganot et al., 2018) (c) Relative sensitivity of ca. 60 human cancer cell lines of the NCI-60 panel to phenolaTi, GI_{50} 4.6 ± 2 µM (equivalent to IC_{50}; the equation for GI_{50} derivatization is given in following reference (Meker et al., 2016)).

In vitro cytotoxicity

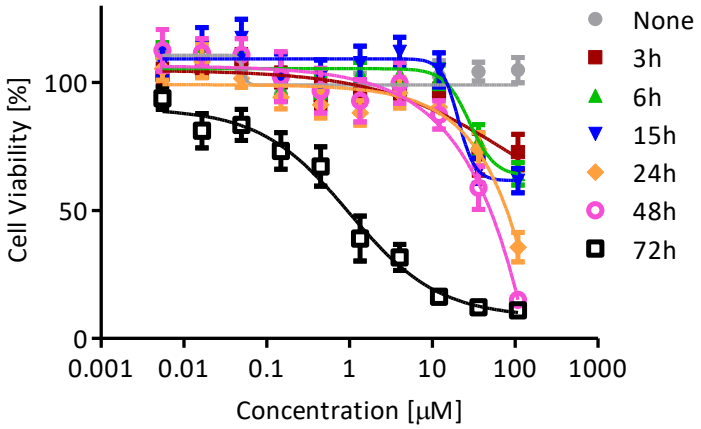

Figure S2: Cytotoxicity curves of phenolaTi. Related to Figure 1. Viability curves of phenolaTi toward human MCF7 breast adenocarcinoma cells using the methylthiazolydiphenyl-tetrazolium bromide (MTT) (Ganot et al., 2013) assay following different incubation times. Relative IC_{50} at 72 hours is 0.65 ± 0.30 µM.

MCF7 cells were selected due to their relative sensitivity to phenolaTi, as deduced from the results previously published on the reactivity toward the NCI-60 panel of the NIH (Meker et al., 2016). The results depict that MCF7 cells were most sensitive to phenolaTi after 72 hours, although some activity was also observed following shorter incubation times. No evident toxicity was observed for at least 6 hours, indicating an anti-neoplastic effect executed through regulated molecular signaling pathways.

Flow cytometry

Cell cycle and apoptosis distribution

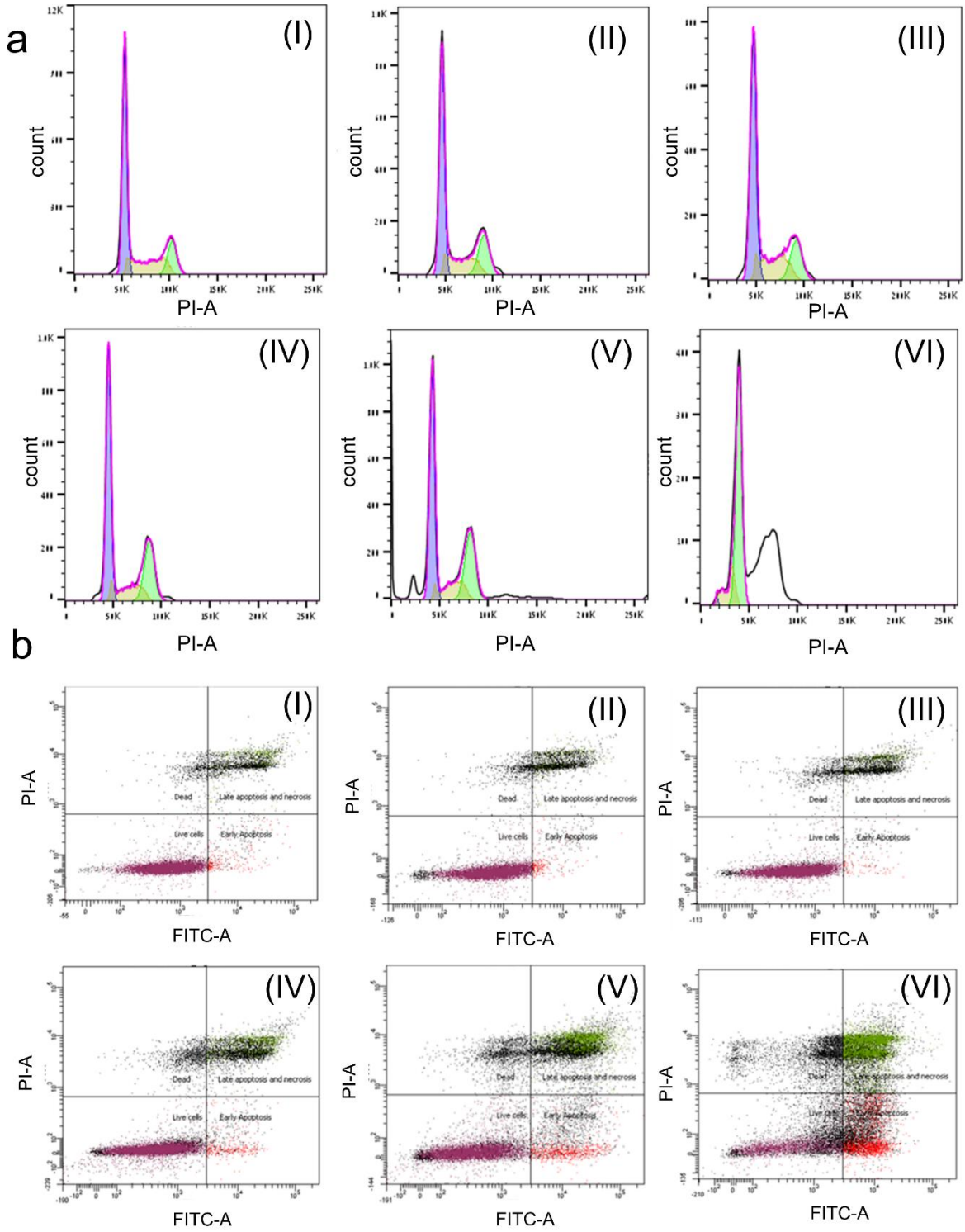

Figure S3: MCF7 cells undergo changes in response to phenolaTi treatment. Related to Figure 2.; (a) Cell cycle distribution following a 54 µM at different time points: (I) control (0 hours- untreated); and after (II) 3 (III) 6 (IV) 15 (V) 24 (VI) 48 hours of incubation (showing one of three repeats). (b) Time dependent effect of phenolaTi at 54 µM on apoptosis in MCF7 cancer cells, as recorded using flow cytometry, (I) control (0

hours- untreated); and after (II) 3 (III) 6 (IV) 15 (V) 24 (VI) 48 hours of incubation (showing one of three repeats).

Short term effect (3-15 h) of phenolaTi

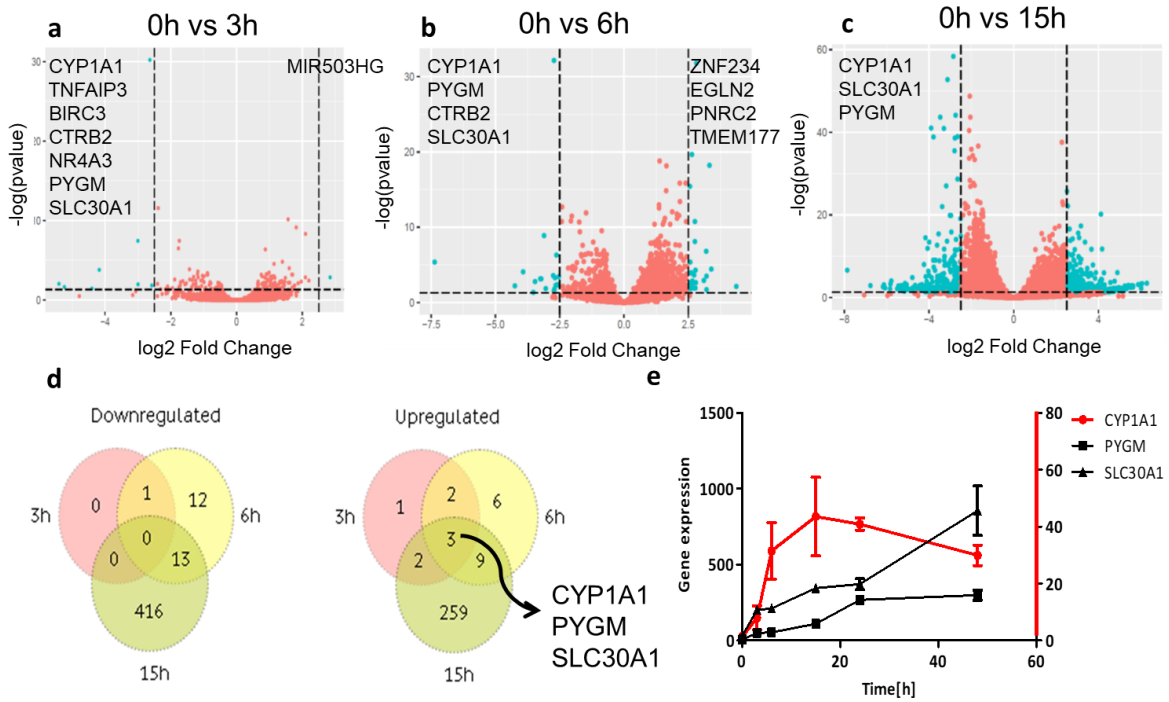

Figure S4: Short term changes in genes expressions after treatment with phenolaTi. Related to Figure 2. (a-c) The volcano plots describe the fold change expression of the genes (x-axis) and the p-value for significant changes in expression (blue dots present significant change, up-left or down-right regulated, between the selected time point and 0- untreated cells) at three time points (a) 3 (b) 6 and (c) 15 hours of exposure relative to control (untreated cells) (d) Venn diagram describes overlap of altered genes at different time points divided into up and down regulated genes (e) Gene expression of CYP1A1, PYGM and SLC30A1 over time.

Nine genes showed significant changes (Q-value< 0.05, and fold change >2) already within 3 hours of exposure, followed by 46 genes at 6 hours, and subsequently 702 genes after 15 hours of incubation. The most significantly altered gene (p-value 4.7e-35) SLC30A1 is associated to cation transmembrane transporters and calcium channel inhibitor activity. Interestingly, upregulations of this and related genes are involved in zinc efflux localized in the endoplasmic reticulum membrane (Barresi et al., 2018). Another significantly upregulated gene is PYGM, an enzyme in carbohydrate metabolism. Of the 46 genes changed within 6 hours, 19 genes were upregulated, and 27 genes were downregulated (Fig. S4a-e); among the downregulated genes, EGLN2 (p-value 4.66e-6) is involved in oxygen sensing related to hypoxia tolerance. Additional downregulated genes are PNRC2 (p-value 5.6e-24) associated with energy balance/storage, and TMEM177 (p-value 2.2e-22) – a mitochondrial respiratory chain complex assembly factor. This gene signature further supports the effect on mitochondria previously observed for related Ti phenolato compounds, accumulated in the mitochondria organelle (Schur et al., 2013). Examining the 702 genes that were changed at 15 hours, 272 were upregulated and 430 downregulated. The downregulated genes relate to cell cycle checkpoints such as CDC23 gene, and DNA damage such as BRCA1 gene. The upregulated genes relate to cellular response to metal ions such as CYP1A1.

CYP1A1 is a member of cytochrome p450 superfamily enzymes, which are involved in drug metabolism and monooxygenase reactions (from NAD(P)H). These proteins are localized mainly in the inner membrane of the mitochondria or the endoplasmic reticulum and are associated with cancer susceptibility (Agúndez, 2004; Brignac-Huber et al., 2016; name Kawajiri et al., 1993; Sharma et al., 2014). CYP1A1 together with PYGM (see above) and SLC30A1 genes (Fig. S4e) are immediately upregulated in response to phenolaTi, stay highly expressed through the short times (3,6,15 hours). PYGM relates to phosphorylase activity in glycogen metabolism (Smutna et al., 2014) and SLC30A1 relates to cellular

metal transport (Guo and Cousins, 2009). Interestingly, two out of three proteins (SLC30A1 and CYP1A1) are functionally related to the endoplasmic reticulum.

Gene Set Enrichment Analysis (Liberzon et al., 2011; Subramanian et al., 2005)

Cluster I

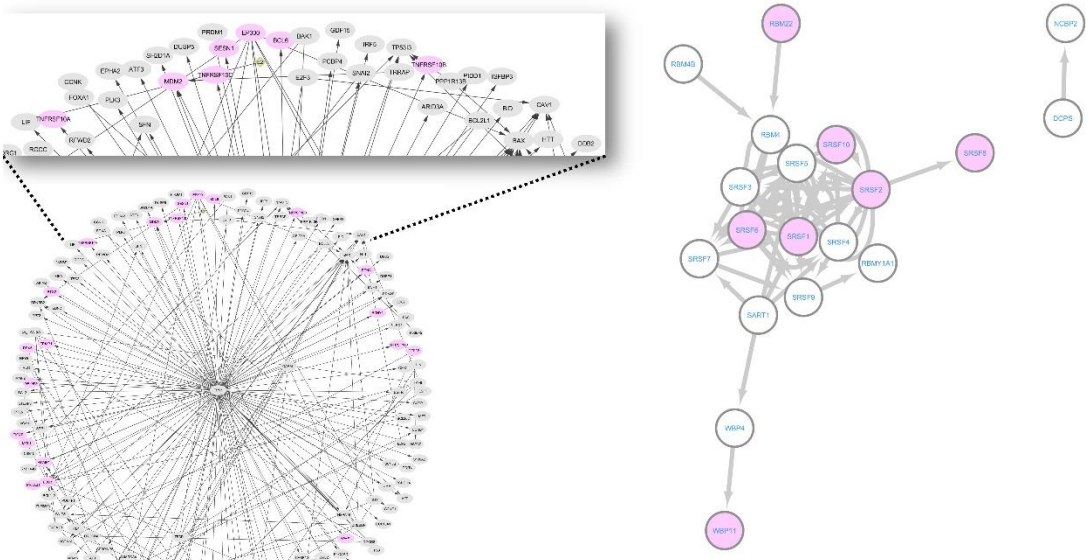

Figure S5: Gene set enrichment analysis using Molecular Signatures Database (MSigDB) for gene expressed in Cluster I. Related to Figure 3. Two representative pathways and our corresponding expressed genes (pink): direct p53 effectors and mRNA cis splicing, via spliceosome pathways.

Cluster II

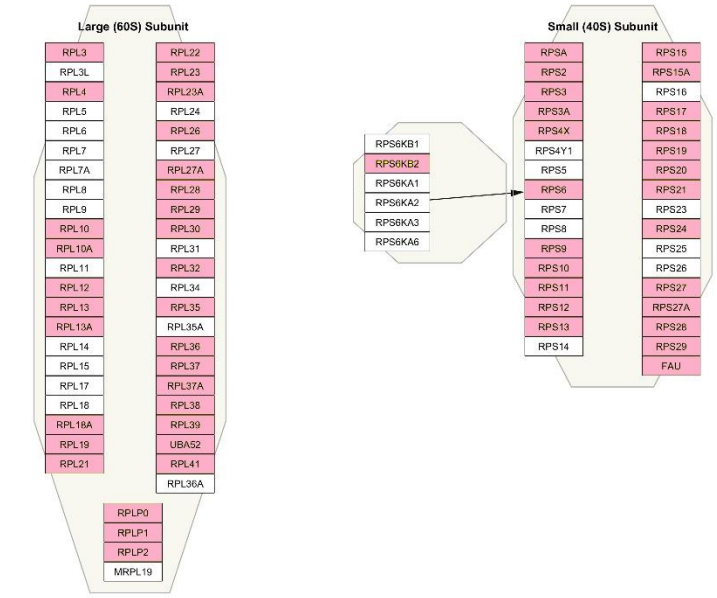

Cytoplasmic Ribosomal Proteins

Figure S6: Gene set enrichment analysis using Molecular Signatures Database (MSigDB) for gene expressed in Cluster II. Related to Figure 3. One representative pathway and our corresponding expressed genes (pink): cytoplasmic ribosomal proteins pathway.

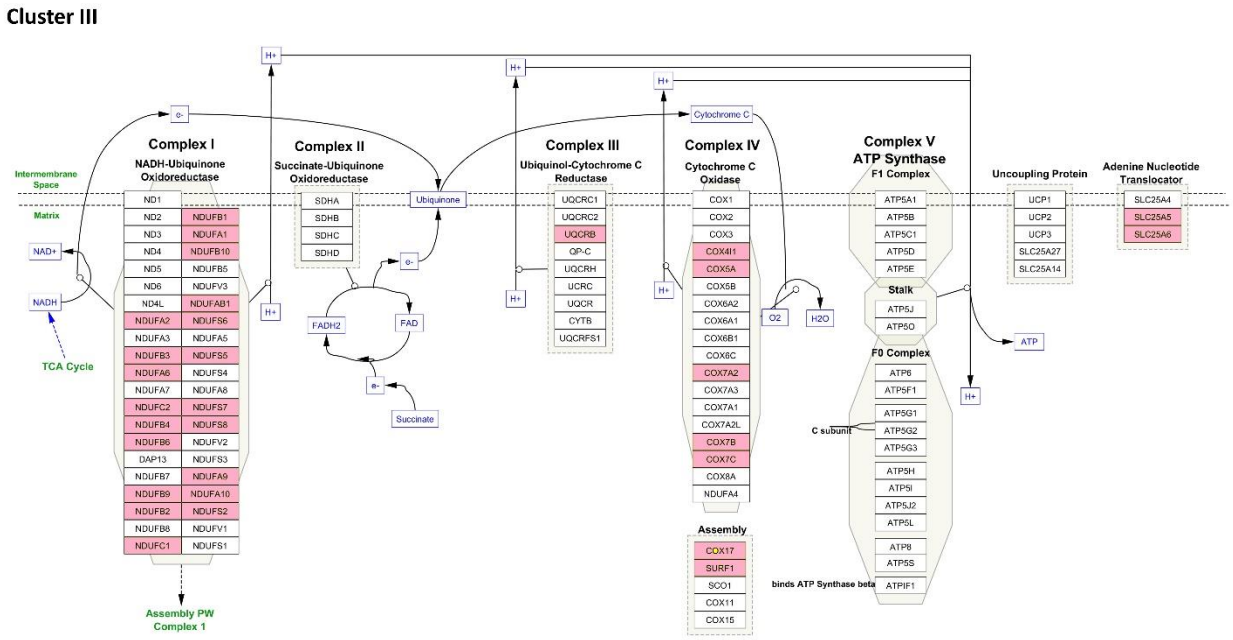

Electron Transport Chain (OXPHOS system in mitochondria)

Figure S7: Gene set enrichment analysis using Molecular Signatures Database (MSigDB) for gene expressed in Cluster III. Related to Figure 3. One representative pathway and our corresponding expressed genes (pink): electron transport chain (OXPHOS system in mitochondria) pathway.

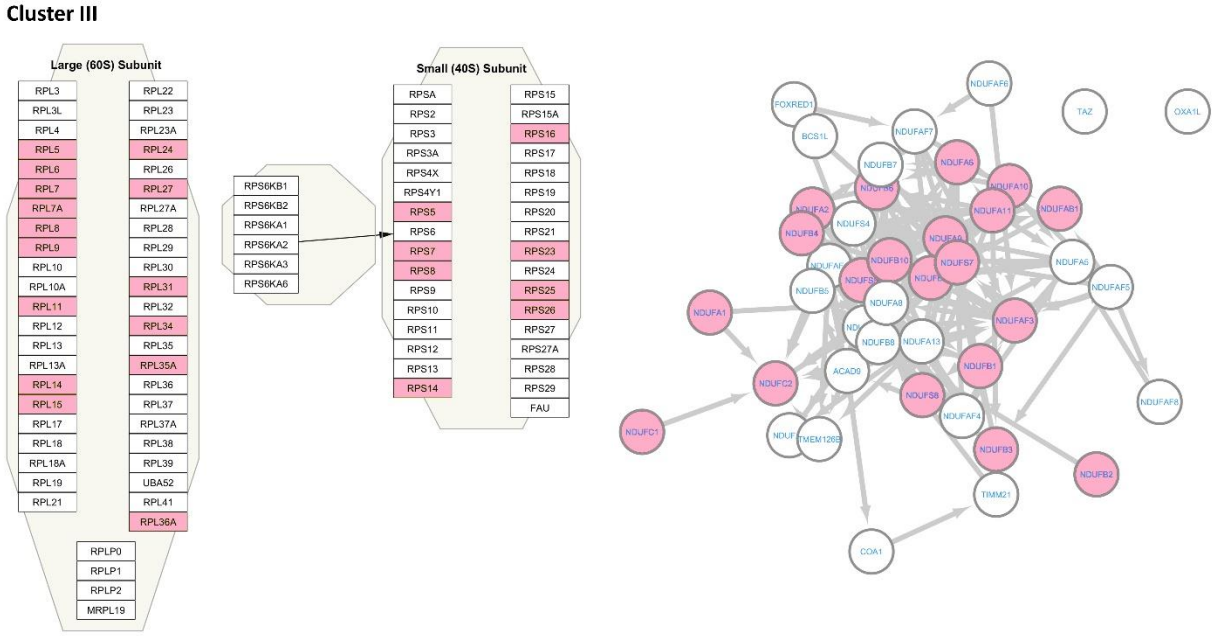

Cytoplasmic Ribosomal Proteins

Mitochondrial respiratory chain complex I

Figure S8: Gene set enrichment analysis using Molecular Signatures Database (MSigDB) for gene expressed in Cluster III. Related to Figure 3. Two additional representative pathways and our corresponding expressed genes (pink): cytoplasmic ribosomal proteins and mitochondrial respiratory chain complex 1 pathways.

Cluster IV

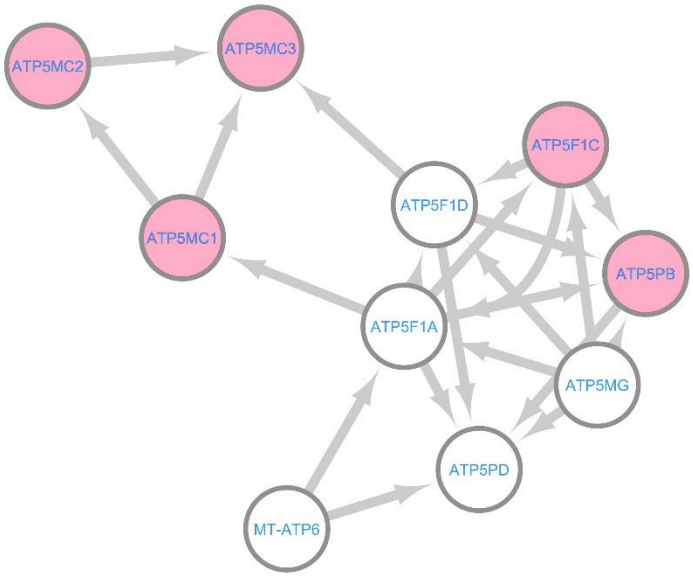

ATP synthesis coupled proton transport

Figure S9: Gene set enrichment analysis using Molecular Signatures Database (MSigDB) for gene expressed in Cluster IV. Related to Figure 3. One representative pathway and our corresponding expressed genes (pink): ATP synthesis coupled proton transport pathway.

Cluster V

Cell cycle G2M phase transition

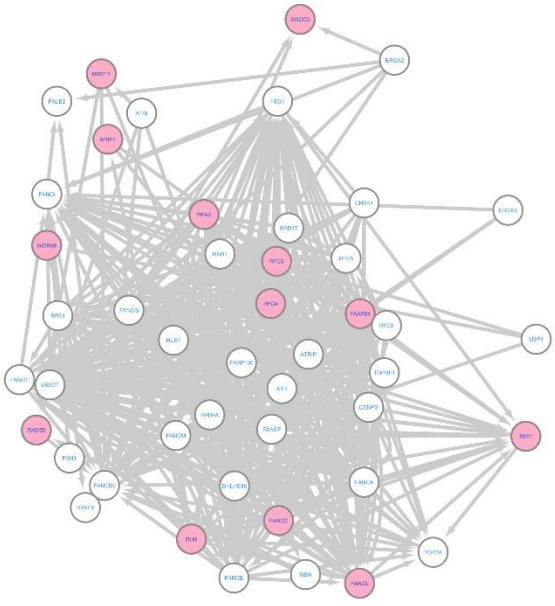

Fanconi anemia pathway

Figure S10: Gene set enrichment analysis using Molecular Signatures Database (MSigDB) for gene expressed in Cluster V. Related to Figure 3. Two representative pathways and our corresponding expressed genes (pink): cell cycle G2/M phase transition and Fanoconi anemia pathways.

Analysis of pathway related genes: PhenolaTi causes changes in hypoxia and endoplasmic reticulum related genes

Endoplasmic reticulum related genes

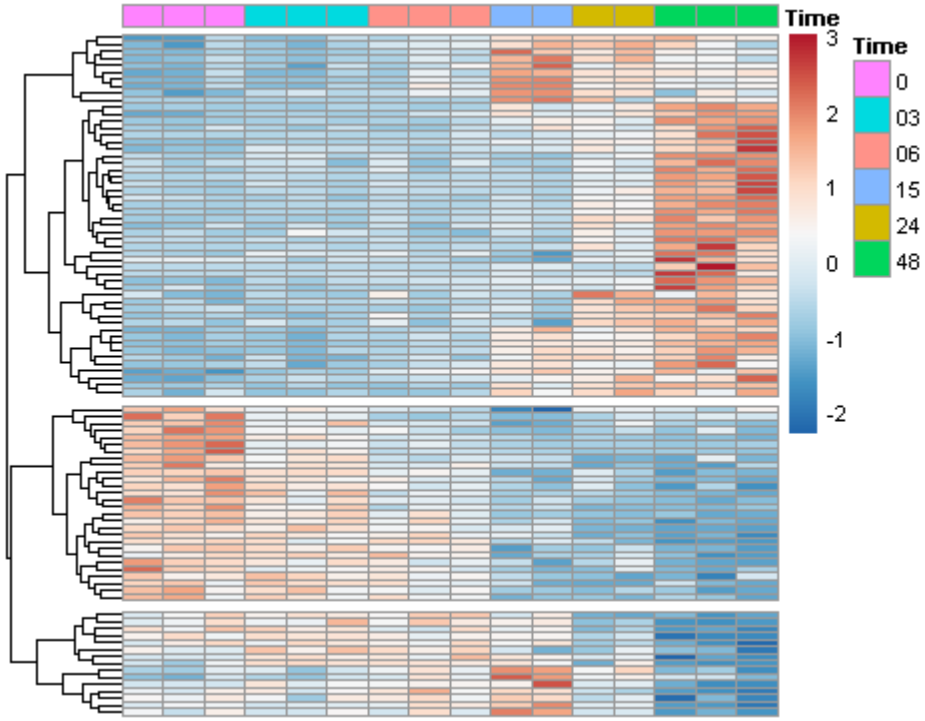

Figure S11: Changes in expression of ER related genes in response to phenolaTi in MCF7 cells at 54 µM. Related to Figure 4. A 95-gene cluster of the total 575 genes previously reported to relate to ER stress (Han et al., 2013); these genes were significantly altered over time in our experiment (p-value < 0.001).

Gene validation- ddPCR

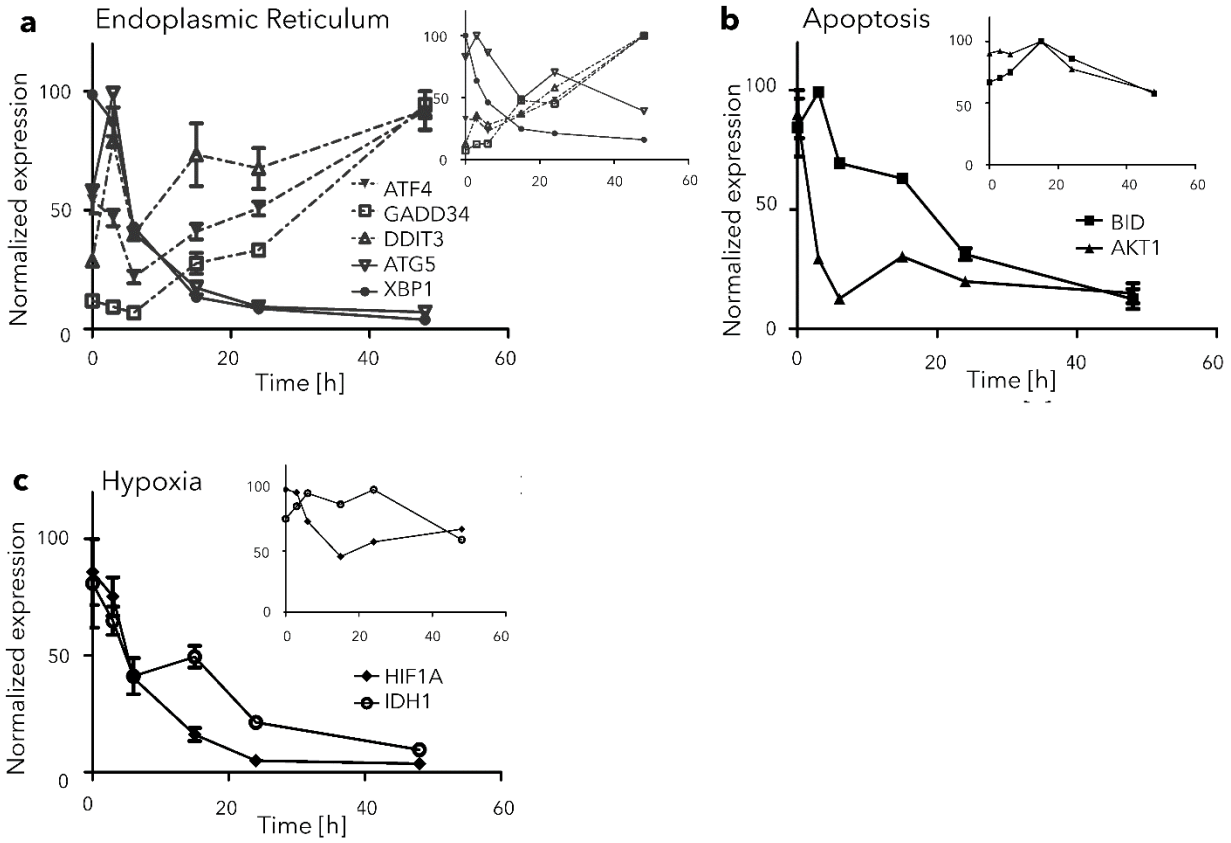

Figure S12: Gene expression alteration in response to phenolaTi in MCF7 cells: RNA-seq correlates with ddPCR results. Related to Figure 4. Cells were treated with 54 µM phenolaTi and sequenced in duplicate after 0 (untreated), 3, 6, 15, 24 and 48 hours. Expression analysis included ddPCR. Normalization was performed relative to the maximal expression of each gene. (a) Five representative genes related to endoplasmic reticulum stress are depicted (ATF4, GADD34, DDIT3, ATG5, XBP1). Upper level (minimized graph) expression illustrates the results obtained through RNA-seq of the corresponding genes. (b) Two representative genes, related to apoptosis are depicted (BID, AKT1). Upper level (minimized graph) expression illustrates the results obtained through RNA-seq of the corresponding genes. (c) Two representative genes, related to hypoxia are depicted (HIF1A, IDH1). Upper level (minimized graph) expression illustrates the results obtained through RNA-seq of the corresponding genes for comparison.

Independent p53 cytotoxicity

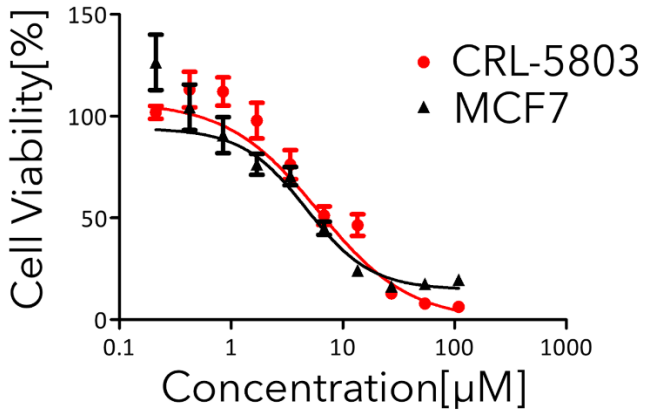

Figure S13: *In vitro* validation assay is independent of p53 cellular status. Related to Figure 5. Cytotoxicity curves of phenolaTi toward human MCF7 and CRL-5803 cancer cells using the MTT assay following 72 hours of incubation, showing similar activity. Relative IC_{50} of phenolaTi on MCF7 and CRL-5803: 4.59±1.78 and 6.66 ± 1.75 μM, respectively.

The cell cycle arrest and altered DNA repair pathways, as well as the apoptotic response, suggest the involvement of TP53. The transcriptomic analysis points to participation of p53 protein in the cellular response to phenolaTi in three main clusters (Fig. 3 cluster (I)/(III)/(V)). Whereas some p53 regulating genes are downregulated (Fig. 3 cluster (V)), such as CHEK2, CDK1 and RAD51, most related genes are upregulated within 15 or 48 hours (Fig. 3 cluster (III)/(I)), among which are GADD45 and BCL6. To measure dependency of the cytotoxic effect of phenolaTi on p53 status, cell viability was compared for two cell lines, based on the methylthiazolydiphenyl-tetrazolium bromide (MTT) assay (Ganot et al., 2013): MCF7 cells with wild type p53 gene (Wasielewski et al., 2006), and CRL-5803 lung carcinoma p53 null-cell line (Blandino et al., 1999) (Supplemental Fig. S7).
Both cell lines responded similarly to the phenolaTi treatment. This result may suggest a p53 independent mode of action of phenolaTi and may point to an alternative DNA-damage and apoptotic-response pathways, e.g. the AKT pathway (Roos et al., 2016). This observation agrees with the cytotoxic effect of phenolaTi on all lines in the NCI-60 panel, comprising both wild type and mutated TP53 cell lines (Supplemental Fig. S1c), as well as with previous reports suggesting upregulation of p53 amounts in response to Ti(IV) phenolato-based compounds (Miller et al., 2016).

Transparent Methods

General: Complex phenolaTi was synthesized according to published procedures (Meker et al., 2016). In all experiments, the compounds were first dissolved in DMSO and then diluted in medium as appropriate.

Cell lines and culture conditions: All experiments were conducted on human MCF7 (breast adenocarcinoma, genetic characterization can be found at https://www.atcc.org/products/all/HTB-22.aspx#specifications, or CRL-5803 (NCI-H1299; lung carcinoma) cells obtained from American Type Culture Collection (ATCC) Inc. Cells were grown in 75-cm^2 culture flasks as adherent monolayer cultures in Dulbecco's Modified Eagle's Medium (DMEM) or Roswell Park Memorial Institute (RPMI) 1640 medium, respectively, supplemented with 10% fetal bovine serum, 1% L-glutamine and 1% penicillin/streptomycin (Biological Industries).

Cytotoxicity: Cells were grown in 96-well plate at density of ~9,000 cells per well, allowed to attach overnight, and incubated for 0 (untreated), 3, 6, 15, 24, 48 and 72 hours with phenolaTi. Then, the MTT assay was applied as previously described (Ganot et al., 2013). Each measurement was repeated at least 3×3 times, namely, three repeats per plate, all repeated three times on different days (9 repeats altogether). Relative IC_{50} values with standard error of means were determined by a nonlinear regression of a variable slope (four parameters) model by the Graph Pad Prism5.0 program.

Experiments conducted on CRL-5803 cells were measured after 72 hours of incubation, according to a published procedure (Ganot et al., 2013).

Experiments conducted with salubrinal (purchased from Sigma) included 70 µM substrate added to the cells, 12 hours prior to addition of phenolaTi, based on previous studies suggesting rapid cellular penetration of phenolaTi (Meker et al., 2016).

Cell cycle analysis: Cells were cultured in a 6-well plate at a density of ~200,000 cells per well and allowed to attach overnight. PhenolaTi was added at a 54 µM concentration and incubated for 0 (untreated)/3/6/15/24/48 hours, such that all samples were harvested at the same time. Cells were trypsinzed and medium was added. The samples were then centrifuged at 2,000 RPM for 5 minutes, washed twice with PBS, and fixed at least overnight in a 1:3 PBS to ethanol solution at 4 ˚C. Cells were then centrifuged at 2,000 RPM for 5 minutes and washed with 0.4 ml PBS. Afterwards, 3.5 µl of RNAse A were added, and the cells were incubated for 15 min at 37 ˚C, stained with propidium iodide at 4 ˚C for 30 minutes, and analyzed by flow cytometry (Becton-Dickinson Excallibar Fluorescence Activated Cell Sorter) using the FlowJo program (Treestar, San Carlos, CA, USA). Each experiment was conducted at least 3 times on different days.

Annexin V/propidium iodide assay: Apoptosis was measured using the Annexin V FITC Apoptosis detection kit (Calbiochem). Cells were cultured in a 6-well plate at a density of ~300,000 cells per well and allowed to attach overnight. PhenolaTi was added at a 54 µM concentration and incubated for 0 (untreated)/3/6/15/24/48 hours, so that all samples were harvested at the same time. All procedures were conducted according to the manufacturer's instructions. The samples were analyzed by flow cytometry (Becton-Dickinson Excallibar Fluorescence Activated Cell Sorter).

Microscopy: Cells were cultured in a 6-well plate at a density of ~300,000 cells per well and allowed to attach overnight. The next day, phenolaTi (54 µM) or DMSO (0.5%) were added and the cells were incubated for 72 hours. The cell response was recorded every 15 minutes for 72 hours by Nikon eclipse-Ti.

RNAseq analysis: RNA was purified from MCF7 cells treated with 54 µM phenolaTi for different incubation periods (0-untreated/3/6/15/24/48 hours), in three biological replicates (one sample each for 15 and 24 incubation time points were omitted) and sequenced using the Cel-Seq2 method (Hashimshony et al., 2016). The results were analyzed as follows: 1) The pair-end samples were demultiplexed as previously published (Hashimshony et al., 2016); 2) Adapters were trimmed by cutadapt; 3) The reads were mapped to the human genome version GRCh38 using STAR (Dobin et al., 2013); 4) The reads were counted by HTseq-count (Anders et al., 2015); 5) The count matrix was normalized to the size of all the libraries analyzed; 6) The z-score of the normalized data was calculated. A one-way ANOVA test was employed to identify the genes that had a similar expression within the biological replicates but the highest

level of variation with the other samples. The results were ordered by their p-values and the top 5,000 genes were selected for in-depth analysis. These genes were clustered into 5 groups according to their expression levels. These groups were analyzed with HOMER (Heinz et al., 2010) in order to find common transcription factors.

ddPCR: The same samples used for RNA-sequencing were used for the ddPCR procedure, employed on the selected genes. Reverse transcription was performed using a cDNA reverse transcript kit (iScriptTM cDNA Synthesis kit; Bio-Rad), according to manufactures instructions. The mRNA expression levels were measured by using QX200Tm Bio-Rad digital droplet PCR. Primers for each gene were purchased from Sigma Aldrich accordingly:

ATF4 (F: AGGAGGAAGACACCCCTTCA, R: ATCGTAAGGTTTGGGACGGG), GADD34 (F: CTGGCTGGTGGAAGCAGTAA, R: TATGGGGGATTGCCAGAGGA), DDIT3 (F: TTCTCTGGCTTGGCTGACTG, R: TCCTCCTCTTCCTCCTGAGC), ATG5 (F: TTTGGTGGAGGCAACCTGAC, R: CCAGCCCAGTTGCCTTATCT), XBP1 (F: TGACATCCAGCAGTCCAAGG, R: GCAAGCCAGGATGCCAAAAA), BID (F: CCAGAACCTACGCACCTACG, R: ACCACATCGAGCTTTAGCCA), AKT1 (F: GGACAAGGACGGGCACATTA, R: CGACCGCACATCATCTCGTA), HIF1A (F: GGCAGCAACGACACAGAAAC, R: TTTTCGTTGGGTGAGGGGAG) and IDH1 (F: ACGGAACCCAAAAGGTGACA, R: GCCAACCCTTAGACAGAGCC).

Polymerase chain reaction (PCR): MCF7 cells were grown in 75-cm^2 cell culture flasks (NuncTM, Thermo Fisher Scientific). About 3x10^6 cells were trypsinzed and DNA was extracted and purified using NucleoSpin® Tissue (Macherey-Nagel), according to the manufacturer's instructions. The DNA concentration was 60 ng/µl. The DNA concentration was set to 0.4 ng/µl, correlating to 20,000 cells. For the PCR protocol, the REDTaq® ReadyMixTM PCR reaction mix (R2523, Sigma Aldrich) was used. The actin gene was used as the housekeeping gene for evaluation of possible interaction. Primers (F:AGACTCTGTCGTGGCAGTTG, R: CAGCTGGTAAGGGGGACTTG) were purchased from Sigma. Cisplatin, doxorubicin and 5-fluorouracil were purchased from Sigma. The concentration used for all tested compounds was 27 and 54 µM, in duplicates; all repeated at least three times.

Immunoblotting assay: Cells were cultured in 6-well plate at density of ~200,000 cells per well and allowed to attach overnight. PhenolaTi was added at 54 µM and the wells were incubated for 16 and 24 hours. Cell protein extracts were obtained by adding Laemmli sample buffer (Bio-Rad, #161-0747) supplemented with 10% β-mercaptoethanol. About 40 µg of total protein (determined by BCA method) was loaded on gradient 4-20% Mini-Protean® TGX Stain-Free protein gel (Bio-Rad), in tris-glycine-SDS running buffer, resolved at 25 mA (per gel) and electroblotted to nitrocellulose or activated polyvinylidene fluoride (PVDF) membrane at Trans-Blot Turbo Transfer system (Bio-Rad). The membranes were blocked with 3% non-fat milk solution in Tris buffered saline and Tween 20 (TBST) for 1 hour at room temperature. Membranes were incubated for overnight at 4 °C with either anti- PERK (1:400, #3192, Cell Signaling), GAPDH (1:400, ab181602, EPR16891, ABCAM), p-EIF2α (1:400, ab32157, E90, ABCAM), ATF4 (1:400, ab184909, EPR18111, ABCAM), p-IRE1 (1:400, ab124945, EPR5253, ABCAM), primary antibody diluted in blocking solution. Membranes were washed and then incubated with peroxidase conjugated secondary antibodies (1:10,000, Sigma) diluted in blocking solution for 1 hour at room temperature. The membranes were washed with TBST and proteins were visualized using enhanced chemiluminescence (ECL) solution (Bio-Rad) using Gel DocTM imaging system (Bio-Rad).

Gene expression (qPCR): Total RNA was extracted from MCF7 cells similarly to RNA-seq analysis. Reverse transcription was performed using iScript cDNA synthesis kit (Bio-Rad), and mRNA expression levels were measured with qPCR. SYBR-Green (Bio-Rad, USA) was used in a CFX-384 Real-Time PCR system (Bio-Rad). Data were analyzed using the ΔΔCt method. Relative quantities of gene transcripts were normalized to actin (same primer as in PCR section). Primers for the spliced variant of XBP1 protein were specifically designed on the 26 base gap differentiated between the long and spliced variants, using the NCBI Primer Blast (F: CTGAGTCCGCAGCAGGTGCAG, R: GAGATACCCAGCTCCGGAACG).

Supplemental References:

Agúndez, J.A.G. (2004). Cytochrome P450 gene polymorphism and cancer. Curr. Drug Metab. *5*, 211–224.

Anders, S., Pyl, P.T., and Huber, W. (2015). HTSeq—a Python framework to work with high-throughput sequencing data. Bioinformatics *31*, 166–169.

Barresi, V., Valenti, G., Spampinato, G., Musso, N., Castorina, S., Rizzarelli, E., and Condorelli, D.F. (2018). Transcriptome analysis reveals an altered expression profile of zinc transporters in colorectal cancer. J. Cell. Biochem. *119*, 9707–9719.

Blandino, G., Levine, A.J., and Oren, M. (1999). Mutant p53 gain of function: differential effects of different p53 mutants on resistance of cultured cells to chemotherapy. Oncogene *18*, 477.

Brignac-Huber, L.M., Park, J.W., Reed, J.R., and Backes, W.L. (2016). Cytochrome P450 organization and function are modulated by endoplasmic reticulum phospholipid heterogeneity. Drug Metab. Dispos. *44*, 1859–1866.

Dobin, A., Davis, C.A., Schlesinger, F., Drenkow, J., Zaleski, C., Jha, S., Batut, P., Chaisson, M., and Gingeras, T.R. (2013). STAR: ultrafast universal RNA-seq aligner. Bioinformatics *29*, 15–21.

Ganot, N., Meker, S., Reytman, L., Tzubery, A., and Tshuva, E.Y. (2013). Anticancer Metal Complexes: Synthesis and Cytotoxicity Evaluation by the MTT Assay. J. Vis. Exp. e50767.

Ganot, N., Briaitbard, O., Gammal, A., Tam, J., Hochman, J., and Tshuva, E.Y. (2018). In Vivo Anticancer Activity of a Nontoxic Inert Phenolato Titanium Complex: High Efficacy on Solid Tumors Alone and Combined with Platinum Drugs. ChemMedChem *13*, 2290–2296.

Guo, L., and Cousins, R.J. (2009). Zinc-regulated ZnT1 (SLC30A1) and Glucocorticoid-regulated ZnT2 (SLC30A2) Influence Zinc Efflux from Pancreatic Acinar Cells.

Han, J., Back, S.H., Hur, J., Lin, Y.-H., Gildersleeve, R., Shan, J., Yuan, C.L., Krokowski, D., Wang, S., and Hatzoglou, M. (2013). ER-stress-induced transcriptional regulation increases protein synthesis leading to cell death. Nat. Cell Biol. *15*, 481.

Hashimshony, T., Senderovich, N., Avital, G., Klochendler, A., de Leeuw, Y., Anavy, L., Gennert, D., Li, S., Livak, K.J., and Rozenblatt-Rosen, O. (2016). CEL-Seq2: sensitive highly-multiplexed single-cell RNA-Seq. Genome Biol. *17*, 77.

Heinz, S., Benner, C., Spann, N., Bertolino, E., Lin, Y.C., Laslo, P., Cheng, J.X., Murre, C., Singh, H., and Glass, C.K. (2010). Simple combinations of lineage-determining transcription factors prime cis-regulatory elements required for macrophage and B cell identities. Mol. Cell *38*, 576–589.

Liberzon, A., Subramanian, A., Pinchback, R., Thorvaldsdóttir, H., Tamayo, P., and Mesirov, J.P. (2011). Molecular signatures database (MSigDB) 3.0. Bioinformatics *27*, 1739–1740.

Meker, S., Braitbard, O., Hall, M.D., Hochman, J., and Tshuva, E.Y. (2016). Specific Design of Titanium(IV) Phenolato Chelates Yields Stable and Accessible, Effective and Selective Anticancer Agents. Chem. Eur. J. *22*, 9986–9995.

Miller, M., Braitbard, O., Hochman, J., and Tshuva, E.Y. (2016). Insights into molecular mechanism of action of salan titanium(IV) complex with in vitro and in vivo anticancer activity. J. Inorg. Biochem. *163*, 250–257.

name Kawajiri, K., Nakachi, K.I., zue Imai, K., Watanabe, J., and Hayashi, S. (1993). The CYP1A1 gene and cancer susceptibility. Crit. Rev. Oncol. Hematol. *14*, 77–87.

Roos, W.P., Thomas, A.D., and Kaina, B. (2016). DNA damage and the balance between survival and death in cancer biology. Nat. Rev. Cancer *16*, 20.

Schur, J., Manna, C.M., Deally, A., Koester, R.W., Tacke, M., Tshuva, E.Y., and Ott, I. (2013). A comparative chemical-biological evaluation of titanium(IV) complexes with a salan or cyclopentadienyl ligand. Chem. Commun. *49*, 4785–4787.

Sharma, K.L., Agarwal, A., Misra, S., Kumar, A., Kumar, V., and Mittal, B. (2014). Association of genetic

variants of xenobiotic and estrogen metabolism pathway (CYP1A1 and CYP1B1) with gallbladder cancer susceptibility. Tumor Biol. *35*, 5431–5439.

Smutna, V., Dieci, M.V., Lefebvre, C., Scott, V., Andre, F., and Fromigue, O. (2014). Is PYGM dysregulation involved in breast cancer cell metabolism.

Subramanian, A., Tamayo, P., Mootha, V.K., Mukherjee, S., Ebert, B.L., Gillette, M.A., Paulovich, A., Pomeroy, S.L., Golub, T.R., Lander, E.S., et al. (2005). Gene set enrichment analysis: A knowledge-based approach for interpreting genome-wide expression profiles. Proc. Natl. Acad. Sci. *102*, 15545–15550.

Wasielewski, M., Elstrodt, F., Klijn, J.G.M., Berns, E.M.J.J., and Schutte, M. (2006). Thirteen new p53 gene mutants identified among 41 human breast cancer cell lines. Breast Cancer Res. Treat. *99*, 97–101.